

# An Improved Algorithm for Reconstruction of the Surface of the Human Body from 3D Scanner Data Using Local B-spline Patches

I. Douros

L. Dekker

B. F. Buxton

Dept. of Computer Science  
University College London  
London WC1E 6BT, UK

## Abstract

*There are an increasing number of applications that require the construction of computerised human body models. The work presented here is a follow-up on a previously presented surface reconstruction algorithm, that has been greatly improved by following a local approach. The advantages of the method are presented, along with explanation of why its results are better compared to the previous algorithm. The result is a compound, multi-segment, and yet entirely smooth and watertight surface. Such a surface has a strong potential of being used for applications of a mainly medical nature, such as calculation of surface area and physical surface reconstruction for prosthetics manufacturing.*

## 1. Introduction

Recent advances in three-dimensional scanning technology have enabled the generation of high-density point data sets that describe the surfaces of real objects, including animate objects such as the human body [3][10]. This means that it is now possible to produce computer-based models that describe in detail the topology and the geometry of an actual human body. Such models can be used to perform fast and accurate automatic measurements. However, such measurements cannot be made on raw point data. A technique must be devised in order to produce a proper surface (skin), given the data. This requires an algorithm that can analyse the data and from it infer the topology (and subsequently the geometry) of the body.

The Department of Computer Science at University College London has been loaned a Body Lines Scanner manufactured by Hamamatsu Photonics [3], capable of

collecting whole body scans in a few (~10) seconds. The scanner's main mechanism consists of 8 cameras, each one measuring reflections from an array of 32 infrared LEDs. The scanner thus captures a 256-point horizontal cross-section of the body every 5 millimetres, as the cameras slide down the approximately 2 metres of the scanner's working height. Data quantity is thus of the order of 301 Kbytes/image (compressed) and its range precision is approximately 12 bits, sufficient to cater for the range accuracy of approximately 2mm in the 1m working width of the machine.

An algorithm is presented that deals with the surface-from-points problem. The problem addressed here is the construction of a surface representation for the body of a specific, real human, using the point data from a scanner. Moreover, this representation must meet the following requirements:

- (i) It must be completely automatic. No user intervention may take place throughout the process.
- (ii) It must be a smooth surface representation, since polygonal meshes are not sufficient for the application domains considered here.
- (iii) It must have the potential of allowing the modelling of tangency discontinuities (cusps) that naturally occur in most human bodies.
- (iv) It must be error tolerant. Outlying and missing data need to be dealt with, so that a surface that describes the whole body is always generated regardless of the size of gaps in the data that occur because of occlusions.
- (v) It must enable easy, reliable and reproducible calculation of whole body volume and surface area.
- (vi) It must be of low computational complexity. The whole process should ideally require only a few minutes of CPU time to calculate.

Requirement (i) necessitates the use of a non-generic algorithm that explicitly assumes that the object to be modelled is a human body in a specific posture [1]. There are a few algorithms that can handle arbitrary topologies (described later in this paper), but the geometric complexity of the human body, together with the requirements of the application areas concerned, indicate that a shape-specific approach should be used in order to exploit the richness of existing information on human body shapes. Requirement (ii) arises from the need for an arbitrary level of surface tessellation so that measurements can be carried out with the maximum accuracy that the hardware can allow. Of course, when it comes to rendering and/or measuring, the surface will have to be polygonised. However, we want a surface description that can generate each time a polygonisation as fine as possible, and in this sense a smooth surface representation is better than a polygon model. In addition, (ii) indicates that some form of the well-established, industry standard B-spline surface models would be appropriate. The approach followed here, to use local patches instead of large surface pieces is partly a result of (iii). This is because local patches can make the modelling of discontinuities easier and they are generally better able to deal with complex topologies such as branchings. Requirements (iv) and (v) arise from the medical nature of the applications considered. Body volume is important for nutritional researchers. From it other important quantities such as fat percentage and body mass index may be measured, thus enabling the diagnosis and treatment of nutritional disorders such as obesity and anorexia. Body surface area is important in particular for determining accurate dosage of medication, especially when the patients are infants and children. Finally, measurement of the surface area for a user-selected part of the body is important for the treatment of burns and for the associated prosthetic and cosmetic surgery treatment.

It must be emphasised, that this paper attempts to address the problem of reconstructing the surface from data given by a specific scanner. Therefore, parts of the body such as the face and hands are not modelled in the same detail as the rest of the body since the specific scanner was not optimised for the modelling of those parts. For face and hands, a combined approach should be followed, using appropriate additional hardware.

## 2. Background

The ‘skinning problem’ (surface from points) is not a new one. Previous attempts fall into two categories: those that require explicit information about the structure of the data points (connectivity), and those that automatically or intelligently infer the structure of the point set from the points themselves.

## 2.1. Previous work on skinning algorithms

The scheme devised by Hughes Hoppe [5] is a generic method for fitting a smooth surface comprised of B-spline patches on unstructured point data of arbitrary topology. It is extremely accurate if given noiseless data without gaps, and also has the advantage that it requires absolutely no prior knowledge of data topology in order to generate the surface. However, the point data generated by the scanner used in this study is not noiseless, and it contains gaps because of occlusions. Hoppe’s algorithm thus cannot be used because it tends to infer incorrect topologies and to join areas of the body that should not be connected, e.g. hands to thighs.

Stoddart and Hilton have also developed a generic surface reconstruction technique, based on the notion of ‘deformable surfaces’ [6]. Their method, which is commonly known as ‘Slime’, generates  $G^1$  continuous deformable surfaces using a generalisation of the concept of biquadratic B-splines. The surfaces produced can describe any surface topology and can accommodate local discontinuities (step edges, roof edges or cusps). The method has low computational complexity and can adaptively generate control points of variable density in order to describe surfaces that are very detailed in some places and very smooth in others. However, the ‘Slime’ method is designed to work well with optimal data sets where noise is low and there are no gaps in the data. Unfortunately, occlusions lead to gaps in the datasets generated by our whole body scanner. Also, the construction of a ‘Slime’ surface implicitly involves manual stages, since the surface quality relies heavily on a user-provided set of voxels, through which topological information can be passed onto the algorithm.

An example of a shape-specific algorithm is the work by Jones et al. [4] for modelling the human torso as a set of key B-spline curves. Although this method can produce a very good representation, it is difficult to extend it in order to cover the whole body. Moreover, it requires intervention of an expert user in order to locate the key slices on the torso, which conflicts with the requirement of full automation in this work.

## 3. Design and methodology

In this section, an overview of the surfaces-from-points algorithm is presented, together with the concepts that have driven the design of the method.

### 3.1 Overview of the proposed algorithm

The main steps of the algorithm are as follows:

- Clean and segment the initial point set.

- Generate a regular point grid (by processing each slice separately and carrying out a data complement process - see section 3.3).
- Resample the regular grid to achieve a robust connectivity.
- Select 4x4 groups of grid points.
- Interpolate each group to generate a set of 4x4 points that defines a patch.

A detailed explanation of each step is presented in the sections that follow.

### 3.2. Assumptions

The surface reconstruction technique proposed is not generic. For it to work, a number of assumptions must be valid. In general, these assumptions have to do with the posture of the body and with the geometrical information that is (or is not) known about it. The set of assumptions is the same as in previous work [1].

### 3.3. Generation of a regular grid of points

The first step of the algorithm is to perform a cleaning process in order to reject points that do not belong to the surface of the body [2]. There are several categories of such points, so the cleaning process consists of several stages. About 40% of all points given by the scanner are low intensity readings due to secondary reflection, and can therefore be easily removed by an intensity thresholding operation throughout the whole data set. Afterwards, points that correspond to the scanner's internal structure are removed. This is a spatial thresholding operation that is also easy, since the locations of the scanner walls are known. A series of more complicated proximity-based operations follow in order to reject the remaining, high intensity outliers.

After cleaning, the point set corresponds well to the body surface. However, it is still unstructured. The operations that follow are necessary in order to infer the structure and topology of the points. Primary landmarks (top of head, seventh cervical vertebra, left and right armpits, crotch, and the ends of the arms and legs) are located first [2], and used to label the data as belonging to the head, torso, left/right legs and left/right arms. After segmentation, the data are converted to local cylindrical co-ordinates, and the medial axes are generated by concatenating the centroid points for each slice of data.

Each body segment is then represented by a  $p \times q$  matrix of vertices;  $p$  is the number of horizontal sample points on the segment, selected to give approximately uniform density across body segments;  $q$  is the vertical dimension of the matrix, which varies according to the length of the segment, based on a uniform, but selectable,

sampling interval. The mesh segments are fitted to the segment data by first binning the points into fixed interval sectors (where the sector angle,  $\theta$ , relates to  $p$ ). Redundant points in each sector are removed by applying a median filter with respect to the radial distance from the segment centroid. Gaps in the matrix are filled by a simple radilinear interpolation. This 'data complement' process imposes an elliptical bias over interpolated areas.

The resulting complete meshes are smoothed using a mean filter, with the window size selected as appropriate for each segment. At the end of this stage, each segment is represented as a deformed cylinder described by a quadmesh. The output of the segmentation is shown in figure 1. We have six primary segments: Left leg, Right leg, Torso, Left arm, Right arm and Shoulders/head (one segment).

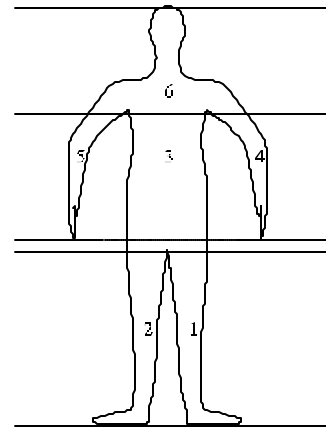
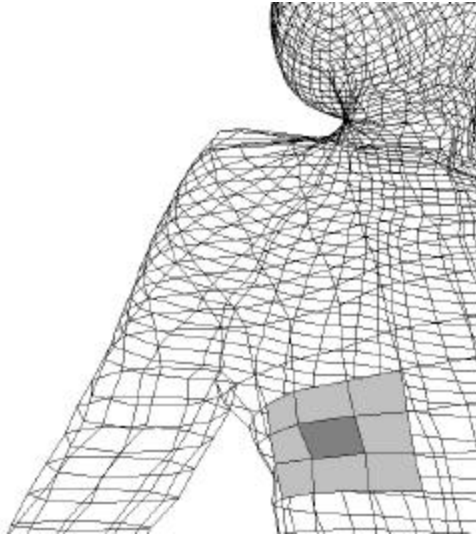


Figure 1: The primary segments of the body

### 3.5. Quadmesh sampling

Once the body is represented as a set of deformed cylindrical quadmeshes, we have an adequate framework for generating a surface. However, it is essential to sample the quadmeshes and use only some of the points for reconstruction. There are two reasons for doing so.

The first reason is that we need to reduce the spatial frequency of grid points, otherwise the noise will produce artefacts on the final surface. To this end, we take samples at uniform intervals along the quadmesh columns. Since the points in each row of the quadmesh have a uniform angular distribution around their centroid, sampling at regular intervals retains this property. We can similarly sample some of the quadmesh rows (which correspond to horizontal slices of the body). In both cases, the quadrilateral connectivity is preserved. The frequency of samples taken is an issue to be addressed according to the applications concerned, and generally constitutes a trade-off between the noise and the level of detail required.



**Figure 2: The completed data mesh (detail)**

The picture shows how the data mesh points are connected around a shoulder area. It can be seen that point connectivity remains consistent around the join. The vertices of the shaded (dark grey) quadrilateral constitute what we define as a 2x2 neighbourhood on the mesh. If we include the vertices adjacent to the light grey shaded areas, this defines a 4x4 neighbourhood on the mesh.

The second reason for sampling is that, in the representation presented in sections 3.3 and 3.4, there are no connectivity constraints between different body segments. For example, the meshes that represent the arms are constructed independently of the meshes that represent the torso. This needs to be resolved, otherwise it is impossible to join the arms with the torso in a seamless manner. To make the connection, samples from both segments are selected and matching pairs established so that a mesh of quadrilaterals covers the whole body, including the branching areas (figure 2). This selection and matching process involves distance proximity and angular proximity criteria, as well as detection of segment intersections around the branching points.

#### 4. Surface fitting

In this section we describe the procedure that generates the surface. The problem breaks down to that of interpolating a third-degree B-spline surface over a quadrilateral of  $m \times n$  points, which is already a well known and established technique [7]. Moreover, the case used here is the degenerate case where  $m = n = 4$ , so we only have to incorporate the degrees of freedom that are present in the description of the standard algorithm, and there is no need to solve a tridiagonal set of equations.

After the resampling of the quadmeshes, we have a compound point vertex of known, generalised quadmesh

connectivity. This means that, although the point set cannot be represented as a matrix of points (it is now a whole body, not a set of independent deformed cylinders), there is still a 4-neighbour structure. Each point has 4 neighbours, which can be called its 'top', 'bottom', 'left' and 'right' neighbours. On our grid, each 2x2 neighbourhood (see fig. 2) can be used for fitting a quadrilateral B-spline patch, with the four corners of the patch coinciding with the four points of the 2x2 neighbourhood.

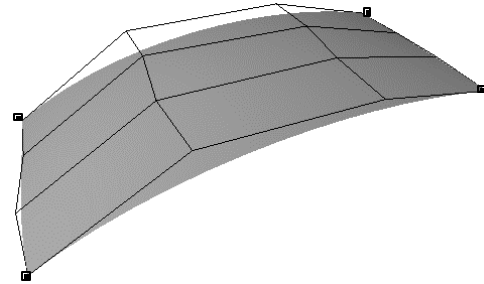


**Figure 3: A patch with its control points**

This is a 2x2 patch of data points  $d_j$  and its 16 control points  $c_k$  lying at the vertices of the 4x4 control grid.

Moreover, we need these patches to join smoothly, thus having  $G^1$  continuity on their boundaries. If we model each patch as a third-degree B-spline patch of 4x4 control points (similar to a Bezier patch), we can achieve this easily, because each one of the 16 control points has an easily understandable, intuitive function. The four corner points define the vertices of the patch, and are the same as the four grid points of the 2x2 neighbourhood. The remaining twelve control points determine the curvature of the patch at the corners ( $3 \text{ control points} \times 4 \text{ corners} = 12$ ), as illustrated in figure 3.

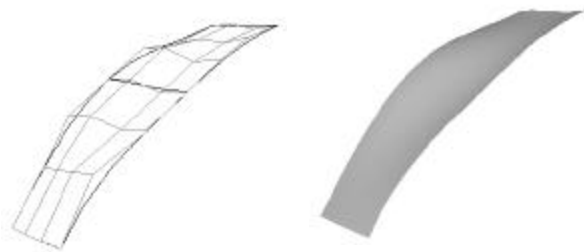


**Figure 4: The joining of two patches**

Left: The boundaries of the patches, along with their control points. It can be seen how the control points along the boundary (bold) form colinear groups perpendicular to the boundary.

Right: The final result, rendered with Phong shading.

In this context, we need to determine the curvature along the boundaries of the patch so that it joins smoothly with neighbouring patches. This is also easy, since the structure of the resampled mesh guarantees that neighbouring patches always join side by side. It is

therefore easy to enforce colinearity constraints between control points of neighbouring patches (figure 4) in order to achieve the desired  $G^1$  continuity between them. However, to determine these colinearity constraints, the  $2 \times 2$  neighbourhood of the grid points is not sufficient. Instead, a broader  $4 \times 4$  neighbourhood around them is used. In other words, the shape of the point set around the area determines the shape of the patch, to make sure that the final surface corresponds to the original object, i.e. the body of the person scanned. Figure 4 demonstrates this. If two B-spline patches join side-by-side, then rows of control points can be treated in a separable manner (as curves) in order to implement the smoothness constraints. A detailed description of these constraints and their implementation can be found in previous work [9].

## 5. Special cases of patches

The interpolation described above is efficient for generating patches that correspond to approximately 95% of the body surface. For the remaining 5% (i.e. the areas around the branchings at the crotch and at the armpits), interpolation has to be carried out in a slightly different manner. In this section, these special cases are described, together with the way in which they are treated.

### 5.1. The bottom of feet

The bottom of the feet is an area completely occluded due to the posture of the subject. Therefore, this area is modelled at the moment as a flat polygon to close the surface and make it watertight. A more satisfactory solution to the problem is left for future work.

### 5.2. The crotch branching

In the case of the branching at the crotch, the problem is that the patches that are immediately adjacent to the branching point have neighbours that belong to different segments. Tangency at their boundaries is therefore more difficult to define. In addition, an inevitable (and natural) discontinuity of tangency in the join between the two leg segments is present at the point of branching. This discontinuity must be modelled explicitly. Thanks to the flexibility of the method, control points can be defined directly using control points from neighbouring patches. The topology of the patches around the branching point can be seen in figure 5.

### 5.3. The armpit branchings

The underarm region branchings are topologically different in comparison to those of the groin. This is mainly owing to the differences in the structure of the

muscles around that area. However, it is still straightforward to define patches (figure 6) so that the armpit shape is covered.

One can see that the patch that is placed directly in the middle of the underarm intersects other patches from the torso and arms. This intersection is useful and can approximately model the skin folds of the armpit - at least as well as can be expected in the absence of data in this highly occluded area. The parts of the patches that lie in the inside of the body (see figure 6) are not visible when the whole body is rendered. Moreover, they are not taken into account when calculating surface area, since they do not constitute parts of the actual body surface.

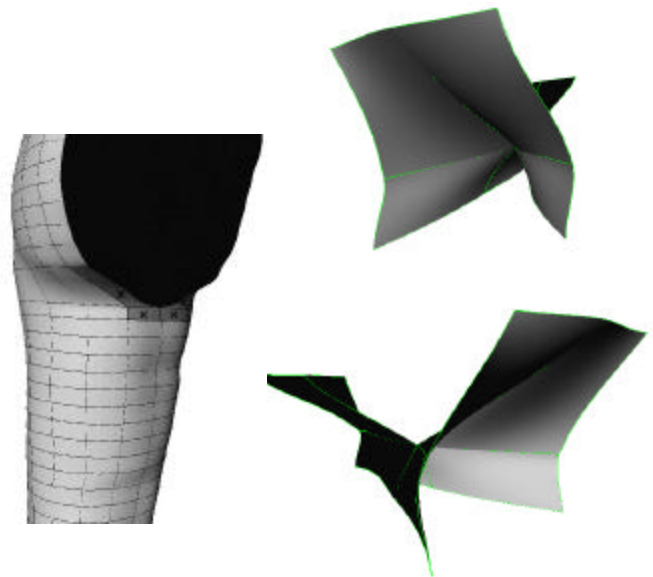


**Figure 5: The modelling of the groin patches**

Left: Detail of the left leg and left half of the torso to show the connectivity. The four marked patches are those immediately adjacent to the branching point.

Right: Two different views of the set of patches that are immediately adjacent to the branching point. The set consists of four patches from each side of the body and is viewed from a front-left (top) and a front-right (bottom) angle.

### 5.4. Top of head and tips of arms

The only problem remaining in order to achieve full body coverage is to cover the top of the head and the tips of the arms. These areas constitute singularities in the otherwise deformed-cylindrical structure of the segments, and therefore quadrilateral patches are inadequate for their modelling. However, the  $4 \times 4$  patches can be used to simulate triangular (trilateral) patches, which can represent the required topology. To simulate a triangular patch, we represent it as a  $4 \times 4$  grid of control points in which all points in the first or last row coincide, as illustrated in figure 7. Interpolation is again driven by

neighbouring points of the quadmesh in order to resolve the singularity that would otherwise occur if the surface segment had more than 4 columns and, because of the singularity, an insufficient/underdetermined set of tridiagonal equations [7] would have to be solved (see appendix). Under such circumstances any reliable linear algebra routine will produce an appropriate error message.

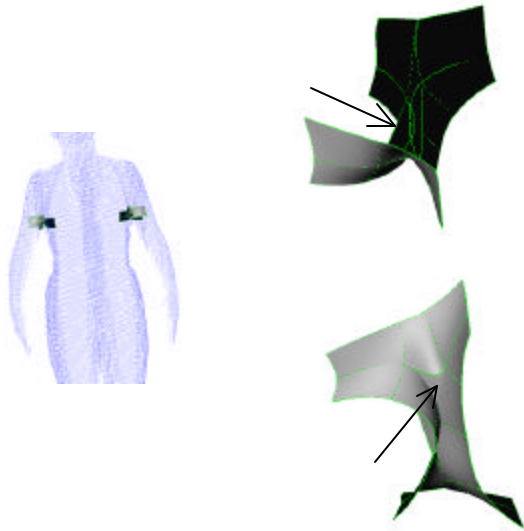


**Figure 6: The modelling of the armpit patches**

Left: The point cloud of a scan together with the two patch sets at the armpit.

Top right: The patch set for the right armpit (from above).

Bottom right: The patch set for the right armpit (from below).

The patch indicated by the arrow on the top right and bottom right pictures is a special patch that extends from the front side of the armpit to the rear in a lateral manner, and is used to close the gap that would otherwise occur.



**Figure 7: The modelling of triangular patches**

The patch illustrated here (together with its control point mesh) is modelled as a degenerate 4x4 quadrilateral patch. Such patches are used to model the top of the head and the tips of the arms (see appendix).

## 6. Results

A body surface produced by the aforementioned

procedures is shown in figure 8. As can be seen, the final surface is smooth and faithful to the original data. Although the surface is generally unaffected by outliers, meaningful details such as the navel are preserved. In fact, the effect of outliers is significantly reduced in comparison to the method described in [1]. Figure 9 shows a comparison of the results obtained by the procedure described, with those obtained previously [1] for an area of the body where an outlier escaped the cleaning procedure. It is nicely demonstrated in figure 9 that the approach presented here is far superior in terms of quality and error tolerance. This is because in the present method an outlying point will only affect the surface locally and, unlike what happened in the previous approach, where large  $p \times q$  quadrilateral splines were used, the error will not propagate throughout the segment.

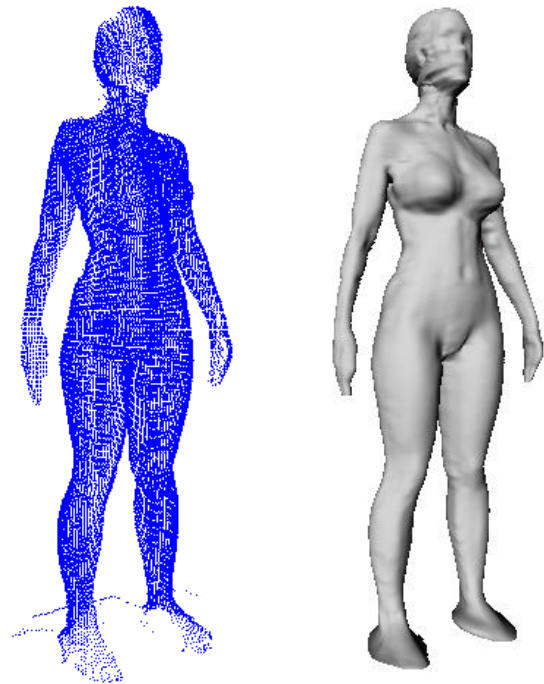


**Figure 8: End result**

Left: The point cloud given by the scanner after cleaning.

Right: The final surface fitted to the point cloud.

All segments join seamlessly and the surface is smooth everywhere. The only features currently lost are the natural cusps at body folds (except in the groin and armpits, where discontinuities are explicitly modelled). However, this works shows that it is now possible to model discontinuities on the surface. To utilise such modelling more generally over the body surface, a method for cusp detection is needed together with a modification of the quadmesh sampling algorithm so that points that correspond to cusps are explicitly marked and sampled in such a manner that they occur at the

boundaries of patches. This is left as future work for the moment. However, its feasibility is now obvious.

Quality is only reduced in the head and face area, but this is expected and is caused by the reduced density of the point cloud around the region. The reason for that is that the LEDs that are coupled to each camera head emit beams in a radial manner (beam spread), so the further the object surface is from the sensors (which is the case for the head), the sparser the captured points will be. In addition, the lowest parts of the feet are not rendered. They were expected to be poorly reconstructed because of the high intensity outliers that appear in the point cloud (figure 8 - left) as the sensors captured part of the scanner's floor.

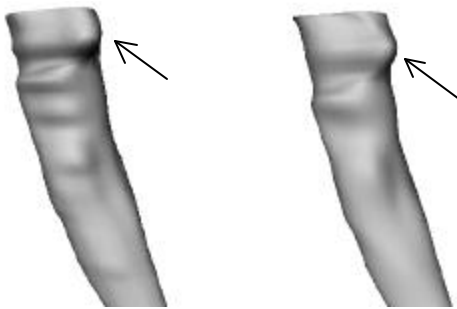


**Figure 9: Comparison of quality**

Left: Part of an arm that includes an obvious outlier, reconstructed using a  $m \times n$  B-spline segment.

Right: The same part of the same arm, this time using the local patch reconstruction approach.

In both cases, the arrow shows the location of the outlier that generated the error. On the first case (left), the error keeps propagating as we move downwards along the arm, whereas in the second case (right), it only affects the patches within the immediate neighbourhood, therefore the rest of the arm is reconstructed correctly.

## 7. Example applications - further work

The system developed can be conveniently used in order to reconstruct the surface of a human body from a cloud of data points. Work is still being carried out in order to verify the accuracy of the method and to determine it in numerical terms, but results so far are very promising. The generated surface representation can be used to calculate the surface area with a precision that is expected to be high enough for medical applications. This does not yet mean that the area measurement coincides exactly with the surface area of the person modelled (at least not until the verification study is complete). However, it is guaranteed that the measurement corresponds exactly to the area of the reconstructed surface. This is because calculation of the area for a B-spline patch using recursive subdivision is a method

already known, straightforward and well-established [7].

The particular way in which the system is designed enables the development of an interface through which the user can manually and intuitively select parts of the body surface. Selection of a set of patches is much easier than trying to trim out a part of a big B-spline segment of arbitrary shape and then trying to calculate a representation for it. This is of interest in the areas of nutritional research and corrective surgery. Selected parts of a surface represented as a set of patches (i.e. as a set of groups of control points) can easily be exported to other CAD applications for further analysis and processing.

Plans for future work also include the development of a parameterised human body model that 'knows' what human bodies look like and makes the fitting more 'intelligent' and robust by allowing a surface to deform in ways that occur within a training set. This involves calculation of Point Distribution Models and Procrustes Analysis, as well as exploitation of previous work [2] for the location of geometrical landmark points on the body, so that a 3D Active Shape Model [8] of the human body shape can be constructed. Development of such a model should enable us to overcome problems with outliers and with missing data in the head and in the lower parts of feet. These problems should be robustly solved for the case of normal subjects (fully articulate and without serious deformities).

## 8. Conclusions

This work has shown that in general, B-spline surfaces are very useful for skinning body scanner data as they enable us to deal with problems of noise, minor artefacts, smooth segment joining and branching topologies. Moreover, it has shown that use of a number of small B-spline patches is significantly better than attempting to wrap one large surface around the object. The current implementation has proven to be successful, and no unexpected problems were encountered. It is also reasonably fast and takes only a few minutes on a 266MHz Pentium II PC with 64MB of memory. This work demonstrates that the surface-from-point-set problem is greatly simplified if the body is first segmented and curves are fitted to subsets of data in order to drive the actual surface patch fitting problem. It also makes it clear that non-generic methods that incorporate assumptions that are related to the structure and geometry of the human body have a strong potential and are appropriate for expansion and further development.

## Acknowledgements

The authors would like to thank Hamamatsu Photonics UK for providing the Body Lines Scanner, as

well as Jonathan Wells and Nigel Fuller from the Dunn Nutrition Research Centre, Addenbrooke's Hospital, Cambridge, for their assistance in the acquisition of volumetric data. They would also like to express their thanks to the anonymous volunteers who offered to have themselves scanned for the purposes of this research. The work presented was funded by the Wellcome Trust and Hamamatsu Photonics.

## APPENDIX: Effecting the triangular patch interpolation

At the top of the head and the tips of arms we need to generate a grid of control points:

$$c_{ij}, i = 0, \dots, 3, j = 0, \dots, 3,$$

equivalent to the 4x4 grids used for the rest of the body skinning, but which can be used to describe a triangular B-spline patch. For the patch to be triangular, the first row of control points must collapse to the same point, i.e:

$$c_{0j} = p, j = 0, \dots, 3$$

This is achieved by carrying out the standard interpolation algorithm [7] over a 4x4 grid of data points:

$$d_{ij}, i = 0, \dots, 3, j = 0, \dots, 3$$

in which, all points of the first *and* second row should collapse to the same point, i.e:

$$d_{ij} = p, i = 0, 1, j = 0, \dots, 3$$

In general, third degree interpolation over a row consisting of  $n$  points  $d_{i0}, d_{i1}, \dots, d_{i,n-2}, d_{i,n-1}$ , where  $d_{i1}$  and  $d_{i,n-2}$  are the endpoints and  $d_{i0}$  and  $d_{i,n-1}$  determine endpoint curvature would produce  $n$  control points  $c_{i,0}, \dots, c_{i,n-1}$ . The pairs of control points at either end of the row:

$$\begin{aligned} c_{i,0} &= d_{i1} \\ c_{i,1} &= a \\ c_{i,n-2} &= b \\ c_{i,n-1} &= d_{i,n-2} \end{aligned}$$

are determined by the data end points  $d_{i1}$  and  $d_{i,n-2}$  and the two degrees of freedom,  $a$  and  $b$ . The latter have to be set explicitly according to application requirements and, in our case, depend on  $d_{i0}$  and  $d_{i,n-1}$ . The remaining control points  $c_{i,2}, \dots, c_{i,n-3}$  are determined by a set of tridiagonal equations that incorporate the above equations and all the remaining data points.

If all data points are the same, and  $n > 4$ , this set of tridiagonal equations is underdetermined and a singularity

occurs. However, if we have exactly four data points, then  $n=4$  and:

$$\begin{aligned} c_{i,0} &= d_{i1} \\ c_{i,1} &= a \\ c_{i,2} &= b \\ c_{i,3} &= d_{i2} \end{aligned}$$

The whole problem has now become explicit, and there is no need to attempt the solution of a set of tridiagonal equations. So, for the first row, we have:

$$c_{0,0} = d_i = p = c_{0,3} = d_{02}$$

and we have also determined that we want  $c_{0j} = p$  for every  $j = 0, \dots, 3$ . We therefore set:

$$a = b = p,$$

all constraints are met and the problem is solved.

## References

- [1] Douros I., Dekker L., Buxton B., "Reconstruction of the surface of the human body from 3D scanner data using B-splines", SPIE proceedings vol. 3640, San Jose, California, January 1999.
- [2] Dekker L., Douros I., Buxton B., Treleaven P., "Building Symbolic Information for 3D Human Body Modeling from Range Data", Department of Computer Science, University College London, March 1999.
- [3] Horiguchi C., 'BL (Body Line) Scanner - The development of a new 3D measurement and reconstruction system', Hamamatsu Photonics, International Archives of Photogrammetry and Remote Sensing, Col. XXXII, Part 5, Hakodate 1998.
- [4] Jones P.R.M., Brooke-Wavell K., West G., 'Format for Human Body Modelling from 3D Body Scanning', HUMAG Research Group, Univ. of Loughborough, International Journal of Science and Technology, Vol.7, No.1, 1995 (pp. 7-16).
- [5] Eck M., Hoppe H., 'Automatic Reconstruction of B-Spline Surfaces of Arbitrary Topological Type', Computer Graphics (SIGGRAPH '96 Proceedings), pages 325-334.
- [6] Stoddart A., Hilton A., Illingworth J., 'Slime : A new deformable surface', Department of Electronic and Electrical Engineering, University of Surrey.
- [7] Piegel L., Tiller W., 'The NURBS book', Second edition, Springer-Verlag Berlin, 1997.
- [8] Cootes T., Taylor C.J., Cooper D.H., Graham J., 'Active Shape Models - Their Training and Application', Computer Vision and Image Understanding Vol. 61, No. 1, January 1995.
- [9] Douros I., 'B-spline surface reconstruction of the human body from 3D scanner data', pp48-52, MRes project report, Department of Computer Science, University College London, 1998.
- [10] Daanen H., Jeroen G., 'Whole body scanners', Displays 19, 1998, pp111-120.